Published in final edited form as:
Mol Biosyst. 2010 July ; 6(7): 1227–1237. doi:10.1039/c001196g.

ANALYSIS OF SITE-SPECIFIC MUTATIONS ON EGFRVIII PHOSPHOTYROSINE SIGNALING NETWORK IDENTIFIES DETERMINANTS GOVERNING U87MG GLIOBLASTOMA CELL GROWTH

Paul H. Huang[1], **Emily R. Miraldi**[2], **Alexander M. Xu**[1,5], **Vibin A. Kundukulam**[1,5], **Amanda M. Del Rosario**[1], **Ryan A. Flynn**[1], **Webster K. Cavenee**[4], **Frank B. Furnari**[4], and **Forest M. White**[1,2,3,6]

[1]Department of Biological Engineering, Massachusetts Institute of Technology, Cambridge, MA 02139

[2]Computational and Systems Biology, Massachusetts Institute of Technology, Cambridge, MA 02139

[3]Koch Institute for Integrative Cancer Research, Massachusetts Institute of Technology, Cambridge, MA 02139

[4]Ludwig Institute for Cancer Research, San Diego Branch and Department of Medicine and Cancer Center, University of California at San Diego, La Jolla, CA 92093-0660

SUMMARY

To evaluate the role of individual EGFR phosphorylation sites in activating components of the cellular signaling network we have performed a mass spectrometry-based analysis of the phosphotyrosine network downstream of site-specific EGFRvIII mutants, enabling quantification of network-level effects of site-specific point mutations. Mutation at Y845, Y1068 or Y1148 resulted in diminished receptor phosphorylation, while mutation at Y1173 led to increased phosphorylation on multiple EGFRvIII residues. Altered phosphorylation at the receptor was recapitulated in downstream signaling network activation levels, with Y1173F mutation leading to increased phosphorylation throughout the network. Computational modeling of GBM cell growth as a function of network phosphorylation levels highlights the Erk pathway as crucial for regulating EGFRvIII-driven U87MG GBM cell behavior, with the unexpected finding that Erk1/2 is negatively correlated to GBM cell growth. Genetic manipulation of this pathway supports the model, demonstrating that EGFRvIII-expressing U87MG GBM cells are sensitive to Erk activation levels. Additionally, we developed a model describing glioblastoma cell growth based on a reduced set of phosphoproteins, which represent potential candidates for future development as therapeutic targets for EGFRvIII-positive glioblastoma patients.

Keywords

Epidermal growth factor receptor; signal transduction; tyrosine phosphorylation; mass spectrometry; computational modeling

[6]Corresponding Author Forest M. White Dept of Biological Engineering MIT, Bldg. 56-787A 77 Massachusetts Ave. Cambridge, MA 02139 617-258-8949 fwhite@mit.edu.

[5]These authors contributed equally to this work.

The authors declare that they have no conflict of interest.

INTRODUCTION

Protein tyrosine phosphorylation is the central mechanism by which receptor tyrosine kinases (RTKs) initiate and propagate critical downstream signaling networks regulating cellular behavior. However, the linkage between specific phosphorylation sites and *in vivo* signaling network activation has yet to be elucidated. The functional role of tyrosine residues on the cytoplasmic tail of the Epidermal Growth Factor Receptor (EGFR) has previously been interrogated either directly by utilizing tyrosine to phenylalanine (Y→F) site-directed mutants *in vivo* or indirectly via *in vitro* methods [1]. To date, *in vivo* studies have been limited to phenotypic characterization of point mutations, while *in vitro* methods often rely on measuring interactions between EGFR phosphopeptide surrogates and potential downstream substrates such as individual proteins or domains, crude cell lysate and more recently, large scale protein domain binding experiments [2-4]. While these *in vitro* approaches are capable of identifying receptor-protein interactions and measuring important biophysical parameters such as binding constants [2], they are conducted under conditions which result in the loss of cellular network information, including regulatory feedback loops that occur downstream of receptor activation, protein localization, and pathway compensatory mechanisms [5]. Previous studies that have attempted to associate *in vivo* phenotypic data from Y→F mutants with *in vitro* binding measurements have often overlooked the point that signaling networks are dynamic entities that have evolved mechanisms to adapt to changes in network structure and utilization that may occur upon point mutation of the EGFR receptor [6].

To address these deficiencies and to complement the data obtained from previous studies, we have employed EGFRvIII, a constitutively active variant of EGFR, as a model system for probing the effects of site-specific tyrosine phosphorylation on intracellular signaling networks. EGFRvIII is expressed in a subset of glioblastoma tumors (GBM, WHO grade IV) and is correlated with poor patient prognosis [7]. A previous investigation of the *in vivo* biological consequences of EGFRvIII mutation determined that Y→F mutations on Y1068, Y1148 and Y1173 of EGFRvIII each resulted in a dramatic decrease in intracranial tumor volume, implicating these sites as critical for tumorigenicity [8]. However, the signaling networks associated with this loss in tumorigenic potential were not explored. In this study, we build on the previous work by utilizing an unbiased mass spectrometric (MS) approach to determine the global phosphotyrosine network effects of six site specific (Y→F) mutations on the EGFRvIII receptor.

Here we show that mutation of any of four phosphorylation sites on the receptor results in a significant change in phosphorylation on most of the other eight sites on the receptor relative to intact EGFRvIII, suggesting intriguing feedback connectivity among the receptor phosphorylation sites. Altered phosphorylation of these sites is functionally significant, as indicated by the effect on tyrosine phosphorylation levels of critical EGFR downstream signaling network components. To identify key sites within these altered networks which regulate cell growth, computational modeling of GBM cell growth as a function of network phosphorylation levels was performed. This analysis identified the Erk pathway as a crucial signaling process regulating EGFRvIII-driven GBM cell behavior, with the surprising finding that Erk1/2 phosphorylation is negatively correlated with cell growth. Genetic manipulation of this pathway supported this finding and demonstrated that EGFRvIII-expressing GBM cells are sensitive to Erk activation levels. Finally, a phosphoproteomic data-driven computational model was developed that is capable of describing GBM cell growth based on a reduced set of molecular determinants.

RESULTS

Cell lines and experimental strategy

To examine how cellular phosphotyrosine-mediated networks are modulated upon the loss of specific tyrosine residues in the cytoplasmic tail of EGFRvIII, we utilized a series of U87MG glioblastoma (GBM) cell lines that were previously engineered to express tyrosine (Y) to phenylalanine (F) EGFRvIII mutants [8]. These mutants are depicted in Figure 1A and consist of four cell lines expressing single mutations at Y845F†, Y1068F, Y1148F and Y1173F, one cell line expressing a double mutation at Y1068F and Y1173F (denoted as DY2) and a final cell line expressing a triple mutation at Y1068F, Y1148F and Y1173F (denoted as DY3). As a control, a previously described cell line expressing the intact EGFRvIII receptor at 2×10^6 copies (U87MG-EGFRvIII) was employed [9].

To minimize confounding cell signaling events associated with growth factors commonly found in serum in cell culture media, the seven cell lines were serum-starved for 24 hours prior to cell lysis and sample preparation. As outlined in Figure 1B, lysates from the seven cell lines were labeled with stable isotopes in 2 different sets of experiments. Each set consists of four cell lines with one cell line (U87MG-EGFRvIII) being used as an overlapping control for the integration of the two datasets. Peptides from the seven samples were stable isotope labeled, mixed, and tyrosine phosphorylated peptides were immunoprecipitated with a mixture of pan-specific anti-phosphotyrosine antibodies. Following immunoprecipitation, phosphorylated peptides were further enriched by immobilized metal affinity chromatography (IMAC) and analyzed by liquid chromatography tandem mass spectrometry (LC-MS/MS). In total, quantitative phosphorylation profiles were generated for two biological replicates with a total of 132 phosphorylation sites on 98 proteins across the seven cell lines (Supplementary Table 1).

Quantitative effects of EGFRvIII site-specific mutations on receptor phosphorylation and downstream signaling networks

In this analysis, we have mapped and quantified nine phosphorylation sites on the EGFRvIII/EGFR receptor, eight on tyrosine residues and one on a serine residue (Figure 2A). As a consequence of the endogenous levels of wildtype EGFR (2×10^5 receptors) expressed in the U87MG cells [10] (note that EGFRvIII is typically found in the context of wtEGFR in EGFRvIII-expressing glioblastomas [7, 11]), figure 2A represents an integrated phosphorylation response of both the EGFRvIII and EGFR receptors. Strikingly, mutation of any single phosphorylation site alters the phosphorylation on most, if not all, other sites on the receptor, with Y845F, Y1068F, and Y1173F demonstrating the largest effects. Single mutation of Y845F resulted in at least a 3-fold decrease in the phosphorylation levels for each of the intact tyrosine/serine residues compared to the control. This general decrease in receptor phosphorylation levels suggests that phosphorylation at Y845 may be required for the optimal activation of the EGFRvIII receptor, consistent with its location in the activation loop of the receptor. Receptor phosphorylation was also strongly negatively affected by single mutations at Y1068F and Y1148F, with each of these mutations causing a decrease in phosphorylation on all remaining phosphorylation sites. The effect of the Y1068F mutation was especially strong, such that the decrease in phosphorylation for many of the sites was greater than that detected for the Y845F mutation. Surprisingly, mutation of Y1173F displayed a dramatically different response compared to mutation of the other three sites, with Y1173F mutation leading to all other sites on the receptor increasing in phosphorylation by at least 1.5-fold relative to the control cells. The DY2 double mutation combines two mutations with opposing effects, as Y1173F led to increased phosphorylation

†Note that the cell line expressing the EGFRvIII Y845F mutant was not included in Huang et al.[8]

while Y1068F gave a strong decrease in phosphorylation. In this combination, the effect of the Y1173F mutation dominates but is diminished, with all remaining sites displaying increased phosphorylation relative to control, albeit to a lesser extent than in the Y1173F cells. The addition of Y1148F, a third point mutation in the receptor, in the DY3 triple mutant abrogated the effect of Y1173F mutation, leading to decreased phosphorylation of the remaining sites on the receptor relative to control cells.

Global analysis of the tyrosine phosphorylation data across the six mutant cell lines revealed similar trends to their receptor phosphorylation profiles, with a large proportion of tyrosine phosphorylation sites downstream of the Y1173F and DY2 mutants exhibiting increased phosphorylation levels relative to control while the remaining mutants (Y845F, Y1068F, Y1148F and DY3) portrayed an overall decrease in network phosphorylation (Figure 2B, full hierarchical cluster with protein names and phosphorylation sites can be found in Figure S1). To determine how each of the EGFRvIII site-specific mutants modulated specific signaling pathways, we mapped the phosphoproteomic data onto the canonical EGFR signaling network (Figure 3). Interestingly, signaling nodes including SHC (Y317), PLC-γ (Y1253), the activation site on STAT3 (Y704/705), a docking site on GAB-1 (Y689), and multiple phosphorylation sites on PI3K were deficient in signal activation in the Y845F, Y1068F, Y1148F and DY3 mutants compared to intact EGFRvIII, while other sites, such as the SFK autophosphorylation site[‡] (Y420) and Erk1/2 activation loop phosphorylation sites (T185/Y187 and T202/Y204) were significantly upregulated in several of these cell lines.

For the Y1173F and DY2 cells, phosphorylation levels of the nodes in the canonical EGFR signaling network tended to reflect the increase in phosphorylation seen at the receptor level, including a stronger increase in the Y1173F cells relative to the DY2 cells. It is interesting to note that increased phosphorylation in these cells also includes the Src and Erk phosphorylation sites. In fact, we initially suspected that the Src and Erk pathways may be activated in selected cell lines to compensate for the loss of signal from the receptor, but their activation in the Y1173F and DY2 cell lines with increased receptor phosphorylation (and increased phosphorylation on the canonical signaling downstream of the receptor) suggests that regulation of these pathways may be more complex than expected, and will require additional studies to elucidate the activation mechanisms in these systems.

Partial least squares regression reveals an anti-correlation between activated Erk1/2 and glioma cell growth

To explore the phenotypic relevance of signaling network adaptations to various point mutations in the receptor, cell growth curves were measured for each cell line (Figure 4A). Contrary to our initial expectations, cell growth among the mutant cell lines appeared to be uncorrelated with tyrosine phosphorylation levels in these cell lines. In fact, despite two of the cell lines displaying increased tyrosine phosphorylation and 4 of the cell lines displaying decreased tyrosine phosphorylation relative to cells expressing intact EGFRvIII, the *in vitro* growth profiles for five of the six mutant cell lines (with the exception of Y1068F, discussed in more detail below) were significantly slower relative to intact EGFRvIII (Figure 4A and Supplementary Methods). Note that this behavior is similar to that seen for murine xenografts of several of these cell lines, which displayed significantly slower xenograft tumor growth rates compared to U87 cells expressing intact EGFRvIII [8]. This divergence between tyrosine phosphorylation levels and cell growth rates implies that cell growth is not simply driven by total tyrosine phosphorylation levels. Instead, the phosphorylation level of

[‡]Note that the peptide containing this phosphorylation site is found in multiple different Src family kinases. Here we have used the numbering scheme for Fyn, as another peptide from Fyn or Yes, was also detected in the analysis.

selected protein components in the context of the overall network may determine U87MG glioblastoma cell growth.

To explore this unexpected divergence further and identify the key regulatory nodes governing cell growth rates, partial least squares regression (PLSR) analysis was used to visualize the relationship between phosphorylation levels of the phosphosites in the MS dataset and cell growth across the mutant EGFRvIII cell lines [12-13]. For this analysis, relative phosphorylation levels of each site were modeled as the underlying, independent-variable block, while quantified GBM cell growth rate constants were modeled as the dependent variable block (calculation of GBM cell growth rate constants from the growth curves is described in Supplementary Methods). Two principle components were sufficient to capture ~90% variance in growth rate constants among the cell lines (Figure S2), defining a 2-dimensional space for projection of both growth rate constants and phosphosite vectors. Projection of growth and those phosphosites that contributed most to principle component axes revealed correlative relationships between phosphosites and growth (Figure 4B). Most saliently, the PLSR-space quadrant negatively correlated (opposite) to growth was enriched for both singly- and doubly-phosphorylated forms of Erk1 and Erk2. Indeed, dramatic fold-changes in the doubly-phosphorylated, active forms of MAP kinases Erk1 and Erk2 correlated negatively with growth (see Figures 4A and 5A), leading us to the non-intuitive hypothesis that further increasing Erk1 and Erk2 activity may inhibit cell growth in U87-EGFRvIII cells.

The active forms of Erk1 and Erk2 exhibit a distinct profile from the majority of canonical EGFR signaling nodes (Figure 3), in which the slower growing mutants (Y845F, Y1148F, Y1173F, DY2 and DY3) demonstrate an up to 4-fold increase in Erk phosphorylation, while the faster growing Y1068F line has both Erk1 and Erk2 phosphorylation on par with the control. The Y1068 residue of both EGFRvIII and wtEGFR has previously been found to interact with the Grb2 adaptor protein and is a direct activator of Erk1/2 via the Sos and Ras pathways [1, 14-15]. It is plausible that inactivation of this site on EGFRvIII prevents recruitment of Grb2 to the receptor, resulting in a decrease in activation of Erk1/2 compared to the other Y→F mutants.

Modulation of the Erk1/2 activation state in U87MG-EGFRvIII cells decreases cell viability

To test the hypothesis that Erk activation negatively regulates cell growth, U87MGEGFRvIII cells were stably transfected to express a constitutively active (CA) form of MEK, in which mutation of two serine residues into aspartate converts MEK into a constitutively active protein [16]. MEK is the upstream kinase activator of Erk1/2; overexpression of CA-MEK in the U87MG-EGFRvIII cells therefore results in hyperactivation of Erk1/2 (Figure 5B). As suggested by the PLSR analysis, increased Erk1/2 activation in the CA-MEK/U87MG-EGFRvIII cells resulted in a 25% decrease in the number of viable cells (Figure 5C). We also set out to determine if the Erk pathway was required for U87MG-EGFRvIII cell growth. U87MG-EGFRvIII cells were transfected with a dominant-negative (DN) mutant of MEK [16], leading to a reduction in active Erk1/2 (Figure 5B). Interestingly, decreasing Erk activation led to 20% decrease in the number of viable cells (Figure 5C) relative to control U87MG-EGFRvIII cells, similar results were obtained following MEK inhibition with U0126 (Figure S3). Taken together, these experiments suggest that GBM cells expressing EGFRvIII are sensitive to modulation of the Erk pathway, and that increasing or decreasing normal Erk activation levels results in a reduction in the number of viable cells.

Experimental validation of glioma cell growth model hypothesis

To provide additional experimental support for our finding that Erk phosphorylation negatively regulates growth in this glioma cell line, we generated stable transfectants of CA-MEK in the six mutant cell lines (Figure S4A). When grown under serum-starvation conditions, CA-MEK mutant cells demonstrated varying viability profiles. The slowest growing cell lines had no significant response to hyperactivation of Erk1/2 (Y1173F, DY2, DY3), while the rest of the EGFRvIII mutants showed sensitivity to increased Erk1/2 phosphorylation (Y1068F, Y1148F and Y845F) (Figure S4B) relative to the control.

To visualize the CA-MEK cell viability measurements in relation to cell line growth rates and phosphorylation levels, we used PLSR analysis once again. Growth rate and CAMEK cell viability measurements were modeled as dependent variables, while phosphosites constituted the independent variable block (Figure 6A). Cell viability under CA-MEK clustered proximal to Erk1/2 phosphorylation and varied inversely with growth rate.

Phosphosite Determinants of Growth

We also used PLSR to develop models of GBM cell line growth as a function of phosphorylation state. To determine which phosphosites were most crucial to modeling growth, a variable importance for projection (VIP) score was calculated for each phosphosite [13]. Without loss in model fitness or prediction, we constructed a “reduced” PLSR model consisting of the thirteen phosphosites with highest VIP score (Figure 6B, 6C). The “reduced” model (R^2=0.9, Q^2=.51) is built on three principle components, and shows predictive improvement over the “full” model (R^2=0.92, Q^2=.17), which includes all 132 phosphosites in the MS dataset. (Figure S5).

DISCUSSION

Receptor and network alterations in response to EGFRvIII site-specific mutations

This study is, to our knowledge, the first comprehensive evaluation of the contribution of EGFRvIII tyrosine phosphorylation sites to intracellular downstream signaling networks. We have demonstrated that EGFRvIII/EGFR phosphorylation profiles fall into two broad categories in response to mutation of critical receptor tyrosine residues (Figure 2A). Mutation at Y845 on EGFRvIII exemplifies the first category, in which a single point mutant leads to a decrease in receptor phosphorylation at multiple other sites, causing a general decrease in overall tyrosine phosphorylation throughout most of the cellular signaling network. It has previously been demonstrated that the Src proto-oncogene phosphorylates EGFR on Y845 and is critical for cell cycle progression and proliferation [17-18]. Accordingly, mutation of the Y845 site on EGFRvIII led to a 1.5-fold decrease in exponential cell growth compared to intact EGFRvIII. The growth defect is accompanied by a decrease in the levels of all 8 phosphorylation sites that were identified on the EGFRvIII receptor, and a concurrent drop in the phosphorylation levels of downstream signaling components in the EGFR network. Single mutation of Y1068F or Y1148F also falls in this category, as does the DY3 triple mutation of Y1173F, Y1068F, and Y1148F. It is interesting to note that the effect of the Y1068F mutation appears to be equal or greater than that seen for the Y845F mutation, as phosphorylation on almost all sites on the receptor is actually lower for the Y1068F mutation compared to the Y845F mutation. The mechanism by which mutation of Y1068F or Y1148F leads to decreased receptor phosphorylation remains to be investigated, but may involve loss of binding of cytoplasmic tyrosine kinases such as Src or Abl, or could be due to a conformational change in the c-terminal region. Although the mechanism has yet to be established, this finding highlights the importance of studying the function of receptor tyrosine phosphosites within the context of the cell. Analysis of the functional roles of post-translational modifications in an *in vitro*

assay cannot fully recapitulate the biological milieu in which receptors normally function and may have obscured the apparent connectivity between Y845/Y1068/Y1148 and other receptor phosphosites that we have uncovered in this study.

The second category of EGFRvIII mutants exhibited an increase in receptor phosphorylation in response to site mutation, as seen for the single mutation at Y1173F and the double mutation at Y1173F/Y1068F. While the mechanism underlying this increase is also still undefined, it is plausible that mutation of Y1173 results in the loss of binding of a negative regulator of receptor phosphorylation; the SHP-1 protein tyrosine phosphatase is one potential candidate. SHP-1 is highly expressed in hematopoietic cells and a closely related isoform of the protein is expressed in epithelial cells[19]. A previous report has shown that SHP-1 binds to wildtype EGFR primarily via the Y1173 site and that Y1173F mutation leads to a decrease in SHP-1-mediated receptor dephosphorylation[20]. Additional studies are required to determine if loss of SHP-1 binding is the predominant mechanism driving increased phosphorylation for the Y1173F and Y1173F/Y1068F double mutation, as other feedback pathways are likely to be contributing as well.

Tyrosine 1173 is a major phosphorylation site on EGFRvIII, responsible for the activation of downstream signaling components through the recruitment of adaptor proteins such as SHC [1, 15]. Intriguingly, loss of Y1173 phosphorylation in the Y1173F mutant led to increased signaling of downstream EGFR canonical signaling network components, including SHC-GAB1-PI3K, STAT3, and PLCγ, indicating that increased phosphorylation on the remaining sites on the receptor was more than sufficient to compensate for the loss of this phosphorylation site. Our data support redundancy in EGFRvIII phosphorylation sites in the activation of downstream signaling pathways, such that multiple tyrosine phosphorylation sites on the receptor may serve to recruit similar adaptor proteins. Such overlap in adaptor binding has been detected during *in vitro* EGFR phosphopeptide interactome experiments [1, 3]. For instance, in addition to Y1173, the adaptor protein SHC has been shown to also bind to Y974, Y1086, Y1114 and Y1148 on EGFR [3], all of which were shown to increase in our phosphorylation study.

Sensitivity of U87MG-EGFRvIII cells to the Erk1/2 activation levels

In a recent study of EGFRvIII signaling networks, we observed that the activation of Erk1/2 increased only slightly with increasing EGFRvIII receptor levels [9]. In light of those findings, we asserted that the EGFRvIII receptor mediates its tumorigenic effect through the preferential utilization of other upregulated pathways (e.g. the PI3K pathway) over the MAPK pathway [9, 21]. Taken together, our current study would suggest that, in addition to the preferential utilization of alternative signaling pathways, the constitutive activation of EGFRvIII may be effectively repressing phosphorylation/activation of Erk1/2. Mutation of specific tyrosine phosphorylation sites on EGFRvIII appears to relieve this repression, resulting in an up to 4-fold increase in Erk1/2 phosphorylation levels (Figures 3 and 5A). Repression of the Erk1/2 pathway by EGFRvIII appears to have functional consequences, as hyperactivation of this pathway in the context of EGFRvIII expression leads to a decrease in viable cell numbers. Consistent with our data, a previous study demonstrated that while MEK activity is 4 fold higher in EGFRvIII expressing fibroblast cells compared to the corresponding cells expressing wildtype EGFR [22], Erk phosphorylation levels remained invariable, even upon the addition of the Erk agonist PMA. In fact, treating EGFRvIII expressing cells with a tyrosine phosphatase inhibitor increased Erk activation, suggesting that the MAPK phosphatase family (MKPs) may be possible candidates for the negative regulation of the MAPK pathway by EGFRvIII [22]. A similar finding was recently made in a mutant, constitutively active, K-Ras^{G12D}-driven colon tumor model where MEK activity is upregulated while phosphorylated Erk levels remain attenuated [23]. The mechanism by which Erk1/2 hyperactivation leads to decreased cell viability remains to be determined, but Erk1/2

attenuation has been reported in the context of other constitutively active tyrosine kinases [24-25].

We have also shown that a minimal activation level of the Erk pathway is required for EGFRvIII driven cell growth, as Erk inhibition results in a decrease in cell viability (Figure 5C). Similarly, in the K-Ras^{G12D} study, treating mice with CI-1040 (an oral inhibitor of MEK) suppressed proliferation in the colonic epithelia [23]. We propose a model in which EGFRvIII fine-tunes the activation of the Erk1/2 pathway (Figure 7): basal activation of Erk1/2 is required for optimal GBM cell growth, but increasing Erk1/2 phosphorylation beyond a particular threshold decreases cell viability. Our data would also imply that the sensitivity of EGFRvIII expressing tumor cells to threshold levels of Erk1/2 activation may be exploited for therapeutic purposes. Glioblastoma patients with PTEN-null, EGFRvIII-positive tumors are refractory to monotherapy with EGFR kinase inhibitors [9, 26]. This poor efficacy plagues a significant population of GBM patients, since ~40% of GBM patients lack the expression of functional PTEN [7]. All of our experiments were performed in the U87MG cell line which is PTEN-null [27]. Given the sensitivity of these EGFRvIII-expressing cells to Erk activation levels, hyperactivation of Erk, through the inhibition of negative regulators such as the MKPs, or Erk inhibition, via the use of MEK inhibitors, may be alternative treatment strategies for EGFRvIII positive, PTEN null patients [28-29].

PLSR analysis as a tool for identification of GBM cell growth determinants

In this work, PLSR enabled visualization of the multivariate phosphorylation network trends in relation to cell growth and led us to generate and experimentally validate an unlikely hypothesis: U87MG GBM cell growth is negatively correlated with Erk1/2 activation. Furthermore, PLSR model reduction selected several other phosphosite nodes in the EGFRvIII signaling network as especially descriptive of growth, and naïve model simulations support that these phosphorylation patterns are correlated with growth in a meaningful way. In addition to Erk1/2 phosphorylation, phosphorylation of Fyn (Y213) was included in the reduced model, with similar VIP score to Erk1/2 phosphorylation. Although the functional consequence of this phosphorylation site is as yet uncharacterized, the tyrosine is located in the SH2 domain (which spans residues 149-246), so may affect the ability of this domain to interact with tyrosine phosphorylation sites, including the auto-inhibitory site (Y531). It is worth noting that protein tyrosine phosphatase receptor type alpha (PTPRA) Y798 was also included in the reduced model. Interestingly, this phosphorylation site has been shown to bind Grb2 and to regulate the ability of PTPRA to dephosphorylate and activate Src and Fyn [30-32]. Together, the Fyn and PTPRa phosphorylation sites implicate a potential role for Src-family kinases in regulating glioma cell growth in U87-EGFRvIII. Tyrosine phosphorylation sites on several metabolic enzymes are also featured in the reduced model, including enolase Y44, phosphoglycerate mutase Y92, and pyruvate kinase M2 (PKM2) Y105. Although PKM2 has recently been shown to bind tyrosine phosphorylated proteins and alter cellular metabolism [33], the function of tyrosine phosphorylation on these three proteins is still uncharacterized. However, the connection between tyrosine phosphorylation of metabolic enzymes and glioblastoma cell growth is intriguing, and further functional studies need to be performed to determine the mechanistic effect of phosphorylation at these sites. Lastly, tyrosine phosphorylation of solute carrier family 38 (SLC38A2 Y41) has previously been identified as a key component in a reduced model of migration and proliferation in human mammary epithelial cells (HMECs) [34]; this phosphorylation site was also correlated with proliferation in the full PLSR model [35]. Although this phosphorylation site is also poorly characterized, its appearance in multiple different growth models may indicate a general role for this protein in regulating growth in multiple different cell types. The identification of these signaling nodes has potential implications in GBM therapy as the combined pharmacological

modulation of the Erk pathway together with any number of these strongly correlated signaling proteins may be required to overcome EGFRvIII-driven GBM cell growth.

EXPERIMENTAL PROCEDURES

Cell Culture, Retrovirus Infection, and Transfection

Human glioblastoma cell line U87MG and engineered U87MG derivatives with the exception of the Y845F mutant have been previously described in [8]. Construction of the Y845F-EGFRvIII mutant cell line, including oligo sequences, is described in the Supplementary Methods. Cells were cultured in DMEM with 10% fetal bovine serum, 2mM glutamine, 100 units/ml penicillin, and 100 mg/ml streptomycin in 95% air/5% CO2 atmosphere at 37°C. U87MG cells expressing EGFRvIII or engineered mutant receptors were selected in 400 μg/ml G418. Stable transfection of MEK mutants (a kind gift from Dr. Chris Marshall, ICR) in U87MG cells is elaborated in detail in the Supplementary methods.

Cell lysis, Protein digestion and Peptide fractionation

U87MG cells were maintained in DMEM medium supplemented with 10% FBS. 1.5×10^6 cells per 10cm plate were seeded for 24 hours, then washed with PBS and incubated for 24 hrs in serum-free media. Cells were lysed in 8M urea as previously described [9]. A small aliquot of each sample was analyzed by micro-BCA (bicinchoninic acid) to provide an approximate normalization for the amount of protein in each sample. More refined normalization occurs through quantification of non-phosphorylated proteins found in the supernatant from the immunoprecipitation (see below). For each of the two biological replicates performed, lysate from three 10cm plates were pooled together. Cell lysate was reduced, alykalyted and digested as previously described [36]. Digested lysate were acidified to pH 3 with acetic acid and loaded onto a C18 Sep-Pak Plus cartridge (Waters). The peptides were desalted (10ml 0.1% acetic acid) and eluted with 10 ml of a solution of 25% acetonitrile and 0.1% acetic acid. Each sample was divided into 5 aliquots and lyophilized to dryness.

iTRAQ labeling of peptides

Lyophilized peptides were subjected to labeling with iTRAQ 4-plex reagent (Applied Biosystems). Each aliquot of peptides was dissolved in 0.5M triethylammonium bicarbonate, pH 8.5 and reacted with two tubes of iTRAQ reagent. The reagents for each of the conditions used were: iTRAQ-114 (U87MG-EGFRvIII), iTRAQ-115 (U87MGY1148F and U87MG-Y1173F), iTRAQ-116 (U87MG-Y1068F and U87MG-DY2) and iTRAQ-117 (U87MG-845F and U87MG-DY3). The mixture was incubated at room temperature for 50 minutes and then concentrated to 30 μl. The four different isotopically labeled samples from each set (outlined in Figure 1B) were combined and acidified with 360 μl of 0.1% acetic acid and then reduced to dryness.

Peptide immunoprecipitation and mass spectrometry

The combined sample was reconstituted with IP buffer (100mM Tris, 100mM NaCl, 1% NP-40, pH 7.4) and incubated with 20 μg of protein G Plus-agarose beads (Calbiochem) and 24 μg of anti-phosphotyrosine antibody (PY100 Cell Signaling Technology and 4G10 Millipore) for 8 hrs at 4°C. The antibody-bead conjugates were then spun down for 5 min at 6000 rpm at 4°C and the supernatant was saved. The beads were then washed prior to elution with 100mM glycine pH 2.5 for 30 min at room temperature. Immobilized metal affinity chromatography (IMAC) was performed to enrich for phosphorylated peptides and remove non-specifically retained non-phosphorylated peptides as previously described [37]. Peptides retained on the IMAC column were eluted with 250mM sodium phosphate (pH 8.0)

and analyzed by electrospray ionization liquid chromatography tandem MS on a QqTof mass spectrometer (QSTAR Elite, Applied Biosystems). MS/MS spectra of the five most intense peaks with 2 – 5 charge states in the full MS scan were automatically acquired in information-dependent acquisition.

Phosphopeptide sequencing and quantification

MS/MS spectra were extracted and searched using MASCOT (Matrix Science). For MASCOT, data was searched against the human non-redundant protein database with trypsin specificity, 2 missed cleavages, precursor mass tolerance of 2.2 amu for the precursor ion and 0.15 for the fragment ion tolerance. Phosphorylation sites and peptide sequence assignments were validated and quantified by manual confirmation of raw MS/MS data. Peak areas of iTRAQ marker ions (m/z 114, 115, 116 and 117) were obtained and corrected according to manufacturer's instructions to account for isotopic overlap. The quantified data was then normalized with values from the iTRAQ marker ion peak areas of non-phosphorylated peptides in the supernatant of the immunoprecipitation (used as a loading control to account for possible variation in the starting amount of sample for each condition). Each condition was normalized against the U87MG-EGFRvIII (114 label) cell line to quantify fold change across all 7 conditions.

Details for biochemical measurements, phenotypic experiments, growth rate calculations, partial least squares regression analysis, and statistical analysis are provided in Supplementary Methods.

CONCLUSION

In summary, phosphoproteomic analysis of EGFRvIII site-specific mutants has led to the discovery of network-wide cellular response to site-specific mutations on EGFRvIII. The response occurs at the level of the receptor, where mutation of any of four tyrosine phosphorylation sites leads to altered phosphorylation on the remaining receptor tyrosine phosphorylation sites, thereby implicating novel interactions among the receptor phosphorylation sites. The changes in receptor phosphorylation are propagated downstream, leading to altered phosphorylation throughout the cellular signaling network, an unexpectedly widespread response to site-specific mutations. Phenotypically, increased or decreased phosphorylation throughout much of the cellular signaling network appears to affect cell growth rate similarly, with five of the six cell lines expressing mutant forms of EGFRvIII growing significantly slower than cells expressing the intact EGFRvIII receptor. To better define the critical nodes regulating cell growth in this complex network, signaling networks and growth rates were correlated, leading to a model where EGFRvIII fine-tunes the activity of the Erk1/2 pathway to optimize cell viability. Experimentally, both hyperactivation and inhibition of the Erk pathway result in a decrease in the viability of U87-EGFRvIII cells. If these results are extensible to xenografts and tumors expressing EGFRvIII, it may be that perturbing Erk1/2 activation in these tumors, through either hyperactivation or inhibition, may lead to decreased tumor growth rates.

Supplementary Material

Refer to Web version on PubMed Central for supplementary material.

Acknowledgments

P.H.H., W.K.C., F.B.F., and F.M.W. designed research; P.H.H., A.M.X., V.A.K., R.A.F., and A.M.D. performed research; E.R.M. conceptualized and performed computational analyses; W.K.C. and F.B.F. contributed new reagents; P.H.H., A.M.X., A.M.D., and F.M.W. analyzed the experimental data; and P.H.H., E.R.M., A.M.D., W.K.C., F.B.F., and F.M.W. wrote the paper.

We thank members of the White laboratory for helpful discussions, Dr. Chris Marshall for the kind gift of the MEK constructs and Dr. Nathan Tedford (MIT) for assistance with the QSTAR Elite mass spectrometer. This work was supported by National Cancer Institute (NCI) Grants U54-CA112967, R01-CA118705, and R01-CA096504 (to F.M.W.), an NCI Integrative Cancer Biology Program Graduate Fellowship (to P.H.H.), a National Science Foundation Graduate Research Fellowship (to E.R.M.), an award from the Goldhirsh Foundation (to F.B.F.), and NIH Grant P01-CA95616 (to W.K.C. and F.B.F.). W.K.C. is a fellow of the National Foundation for Cancer Research.

Abbreviations

GBM	Glioblastoma
EGFR	Epidermal growth factor receptor
LC-MS/MS	liquid chromatography tandem mass spectrometry
RTK	receptor tyrosine kinase
IMAC	immobilized metal affinity chromatography
PLSR	partial least squares regression

REFERENCES

1. Batzer AG, Rotin D, Urena JM, Skolnik EY, Schlessinger J. Molecular and cellular biology. 1994; 14:5192–5201. [PubMed: 7518560]
2. Jones RB, Gordus A, Krall JA, MacBeath G. Nature. 2006; 439:168–174. [PubMed: 16273093]
3. Schulze WX, Deng L, Mann M. Molecular systems biology. 2005; 1:0008. 2005. [PubMed: 16729043]
4. Songyang Z, Shoelson SE, McGlade J, Olivier P, Pawson T, Bustelo XR, Barbacid M, Sabe H, Hanafusa H, Yi T, et al. Molecular and cellular biology. 1994; 14:2777–2785. [PubMed: 7511210]
5. Amit I, Citri A, Shay T, Lu Y, Katz M, Zhang F, Tarcic G, Siwak D, Lahad J, Jacob-Hirsch J, Amariglio N, Vaisman N, Segal E, Rechavi G, Alon U, Mills GB, Domany E, Yarden Y. Nature genetics. 2007; 39:503–512. [PubMed: 17322878]
6. Amit I, Wides R, Yarden Y. Molecular systems biology. 2007; 3:151. [PubMed: 18059446]
7. Furnari FB, Fenton T, Bachoo RM, Mukasa A, Stommel JM, Stegh A, Hahn WC, Ligon KL, Louis DN, Brennan C, Chin L, DePinho RA, Cavenee WK. Genes & development. 2007; 21:2683–2710. [PubMed: 17974913]
8. Huang HS, Nagane M, Klingbeil CK, Lin H, Nishikawa R, Ji XD, Huang CM, Gill GN, Wiley HS, Cavenee WK. The Journal of biological chemistry. 1997; 272:2927–2935. [PubMed: 9006938]
9. Huang PH, Mukasa A, Bonavia R, Flynn RA, Brewer ZE, Cavenee WK, Furnari FB, White FM. Proceedings of the National Academy of Sciences of the United States of America. 2007; 104:12867–12872. [PubMed: 17646646]
10. Nishikawa R, Ji XD, Harmon RC, Lazar CS, Gill GN, Cavenee WK, Huang HJ. Proceedings of the National Academy of Sciences of the United States of America. 1994; 91:7727–7731. [PubMed: 8052651]
11. Ohgaki H, Kleihues P. Am J Pathol. 2007; 170:1445–1453. [PubMed: 17456751]
12. Janes KA, Yaffe MB. Nat Rev Mol Cell Biol. 2006; 7:820–828. [PubMed: 17057752]
13. Kumar N, Wolf-Yadlin A, White FM, Lauffenburger DA. PLoS computational biology. 2007; 3:e4. [PubMed: 17206861]
14. Li N, Batzer A, Daly R, Yajnik V, Skolnik E, Chardin P, Bar-Sagi D, Margolis B, Schlessinger J. Nature. 1993; 363:85–88. [PubMed: 8479541]
15. Prigent SA, Nagane M, Lin H, Huvar I, Boss GR, Feramisco JR, Cavenee WK, Huang HS. The Journal of biological chemistry. 1996; 271:25639–25645. [PubMed: 8810340]
16. Cowley S, Paterson H, Kemp P, Marshall CJ. Cell. 1994; 77:841–852. [PubMed: 7911739]
17. Boerner JL, Biscardi JS, Silva CM, Parsons SJ. Molecular carcinogenesis. 2005; 44:262–273. [PubMed: 16167350]

18. Maa MC, Leu TH, McCarley DJ, Schatzman RC, Parsons SJ. Proceedings of the National Academy of Sciences of the United States of America. 1995; 92:6981–6985. [PubMed: 7542783]
19. Banville D, Stocco R, Shen SH. Genomics. 1995; 27:165–173. [PubMed: 7665165]
20. Keilhack H, Tenev T, Nyakatura E, Godovac-Zimmermann J, Nielsen L, Seedorf K, Bohmer FD. The Journal of biological chemistry. 1998; 273:24839–24846. [PubMed: 9733788]
21. Huang PH, Cavenee WK, Furnari FB, White FM. Cell Cycle. 2007; 6:2750–2754. [PubMed: 17986864]
22. Montgomery RB, Moscatello DK, Wong AJ, Cooper JA, Stahl WL. The Journal of biological chemistry. 1995; 270:30562–30566. [PubMed: 8530489]
23. Haigis KM, Kendall KR, Wang Y, Cheung A, Haigis MC, Glickman JN, Niwa-Kawakita M, Sweet-Cordero A, Sebolt-Leopold J, Shannon KM, Settleman J, Giovannini M, Jacks T. Nature genetics. 2008; 40:600–608. [PubMed: 18372904]
24. Charest A, Wilker EW, McLaughlin ME, Lane K, Gowda R, Coven S, McMahon K, Kovach S, Feng Y, Yaffe MB, Jacks T, Housman D. Cancer research. 2006; 66:7473–7481. [PubMed: 16885344]
25. Kamikura DM, Khoury H, Maroun C, Naujokas MA, Park M. Molecular and cellular biology. 2000; 20:3482–3496. [PubMed: 10779338]
26. Mellinghoff IK, Wang MY, Vivanco I, Haas-Kogan DA, Zhu S, Dia EQ, Lu KV, Yoshimoto K, Huang JH, Chute DJ, Riggs BL, Horvath S, Liau LM, Cavenee WK, Rao PN, Beroukhim R, Peck TC, Lee JC, Sellers WR, Stokoe D, Prados M, Cloughesy TF, Sawyers CL, Mischel PS. The New England journal of medicine. 2005; 353:2012–2024. [PubMed: 16282176]
27. Furnari FB, Lin H, Huang HS, Cavenee WK. Proceedings of the National Academy of Sciences of the United States of America. 1997; 94:12479–12484. [PubMed: 9356475]
28. Jeffrey KL, Camps M, Rommel C, Mackay CR. Nature reviews. 2007; 6:391–403.
29. Roberts PJ, Der CJ. Oncogene. 2007; 26:3291–3310. [PubMed: 17496923]
30. den Hertog J, Tracy S, Hunter T. EMBO J. 1994; 13:3020–3032. [PubMed: 7518772]
31. Hao Q, Rutherford SA, Low B, Tang H. Mol Pharmacol. 2006; 69:1938–1944. [PubMed: 16505154]
32. Maksumova L, Wang Y, Wong NK, Le HT, Pallen CJ, Johnson P. J Biol Chem. 2007; 282:20925–20932. [PubMed: 17507376]
33. Christofk HR, Vander Heiden MG, Wu N, Asara JM, Cantley LC. Nature. 2008; 452:181–186. [PubMed: 18337815]
34. Kumar N, Wolf-Yadlin A, White FM, Lauffenburger DA. PLoS Computational Biology. 2007; 3:e4. [PubMed: 17206861]
35. Wolf-Yadlin A, Kumar N, Zhang Y, Hautaniemi S, Zaman M, Kim HD, Grantcharova V, Lauffenburger DA, White FM. Mol Syst Biol. 2006; 2:54. [PubMed: 17016520]
36. Joughin BA, Naegle KM, Huang PH, Yaffe MB, Lauffenburger DA, White FM. Molecular bioSystems. 2009; 5:59–67. [PubMed: 19081932]
37. Kim JE, Tannenbaum SR, White FM. J Proteome Res. 2005; 4:1339–1346. [PubMed: 16083285]

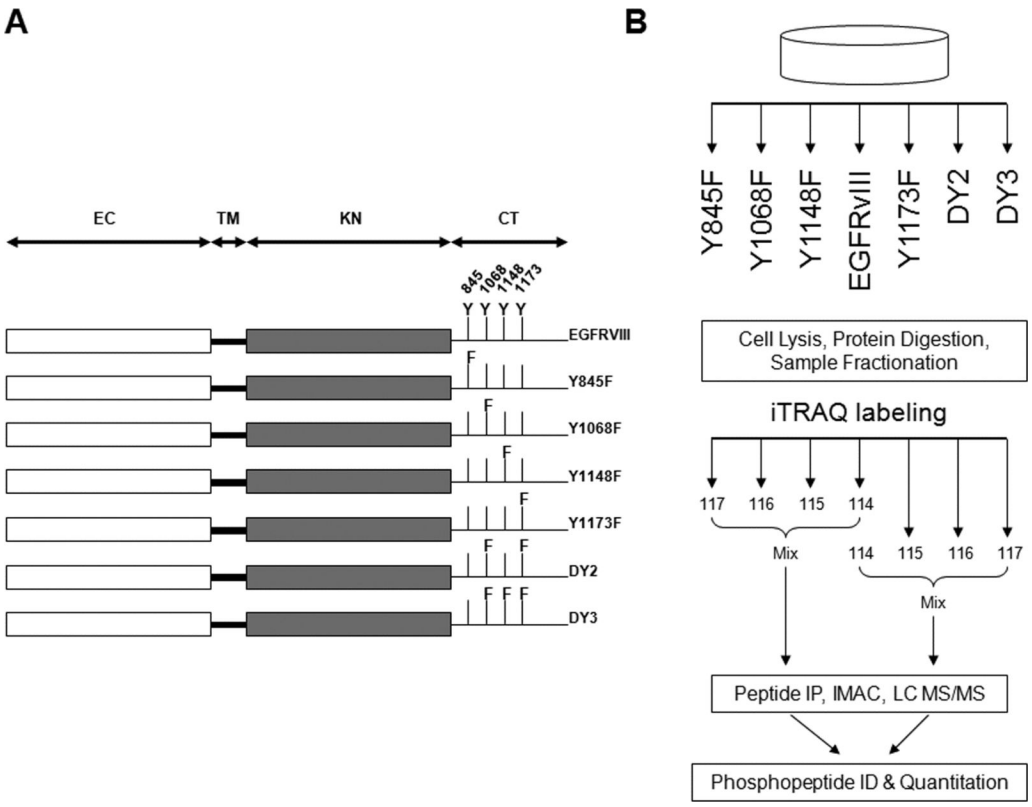

Figure 1. Mutant EGFRvIII receptors and experimental strategy

(A) Six site-directed mutants of EGFRvIII were examined in this phosphoproteomic analysis. Y = tyrosine residue and F = mutation of an existing tyrosine residue to phenylalanine. EC = extracellular region, TM = transmembrane domain, KN = kinase domain and CT = cytoplasmic tail. (B) Outline of MS-based experimental strategy. Samples were labeled with iTRAQ isobaric reagent in two sets of experiments, each consisting of 3 mutant cell lines and U87MG-EGFRvIII. U87MG-EGFRvIII (label 114) was used as a normalization point to integrate both data sets together.

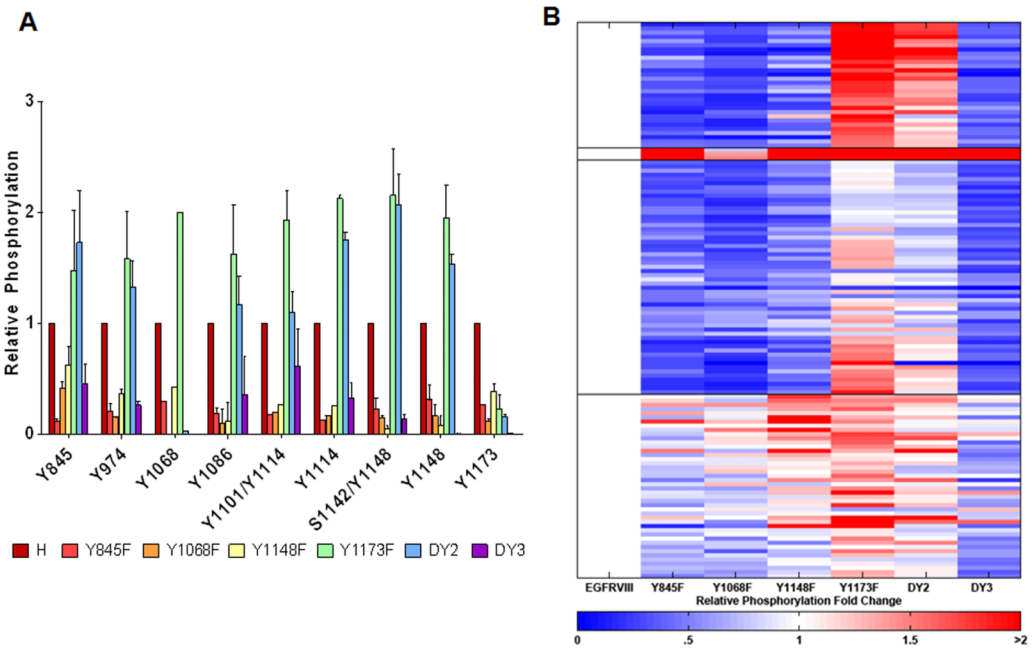

Figure 2. EGFRvIII/EGFR receptor and network phosphorylation

(A) Relative quantification of EGFRvIII/EGFR phosphorylation sites across the mutant cell lines. Phosphorylation levels were normalized relative to the U87MG-EGFRvIII (control) cell line with error bars representing phosphorylation sites that appeared in both biological replicate analyses. (B) Heat map of 132 phosphorylation sites that were quantified in the phosphoproteomic analysis. Phosphorylation levels were normalized relative to the U87MG-EGFRvIII control cell line.

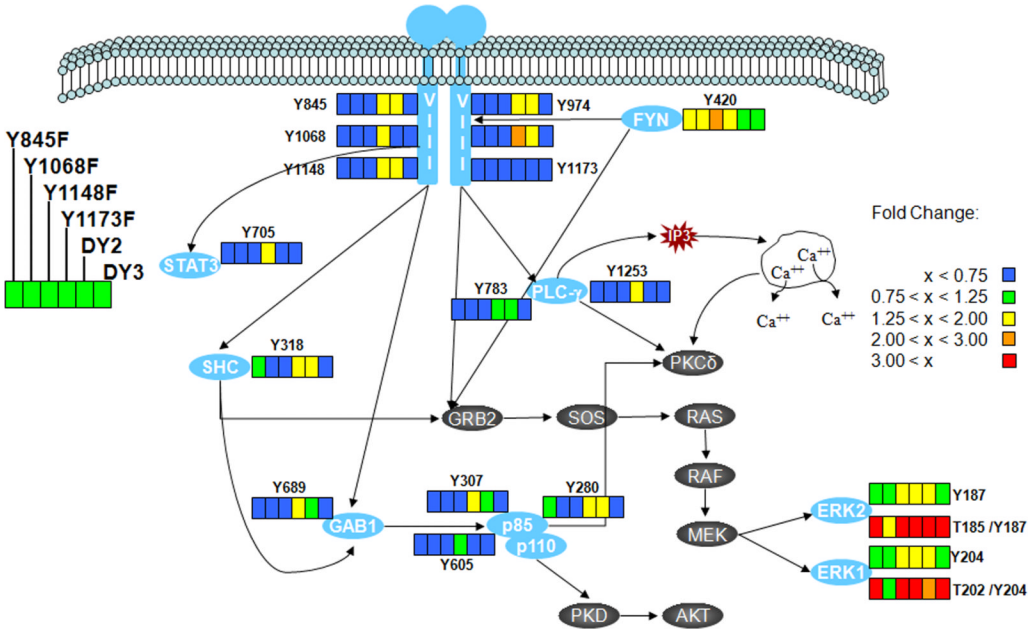

Figure 3. Effect of site-specific EGFRvIII mutations on phosphorylation sites within the EGFR network

Visualization of the fold change in phosphorylation levels in the canonical EGFR signaling network as a function of EGFRvIII site-specific tyrosine residue mutants. Phosphorylation levels are normalized to that of the U87MG-EGFRvIII control cell line.

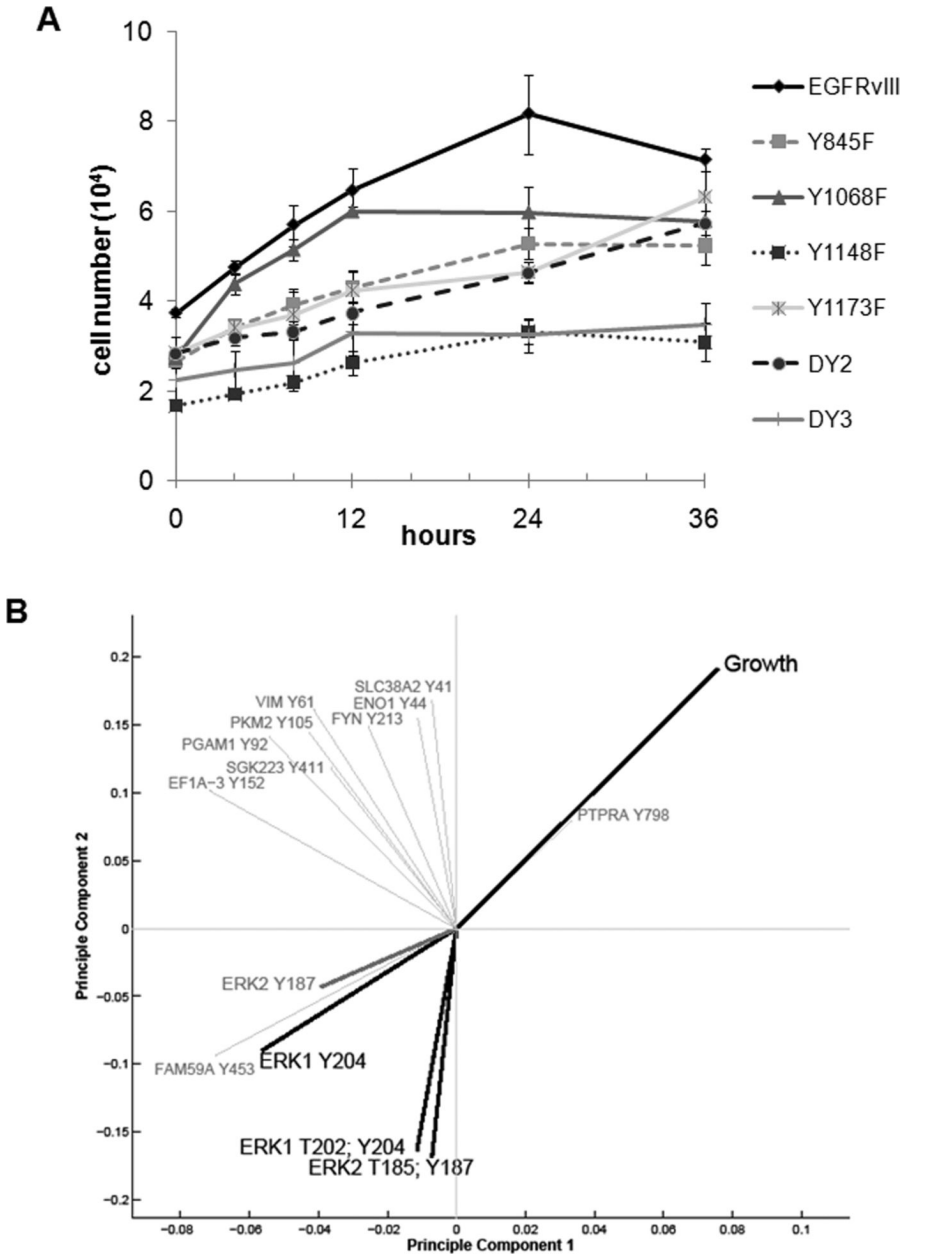

Figure 4. Cell growth rates for EGFRvIII mutant lines and PLSR analysis

(A) Viable cells were counted at 0, 4, 8, 12, 24, and 36 hours to establish cell growth rates for each of the mutant cell lines compared to the wtEGFRvIII expressing cells. The average cell number + the SE from four independent experiments performed in triplicate is graphed. (B) Contributions of growth rate constants and phosphorylation sites to the 2DPLSR principle component axes. The PLSR model identifies phosphorylation sites most descriptive of GBM cell growth rate; those with variable importance for projection > 1.5 (see text) are plotted in the figure. Erk3 Y187 is not included in the reduced model, but, similarly to the other Erk1/2 phosphorylation sites, is in the PLSR quadrant negatively correlated with growth.

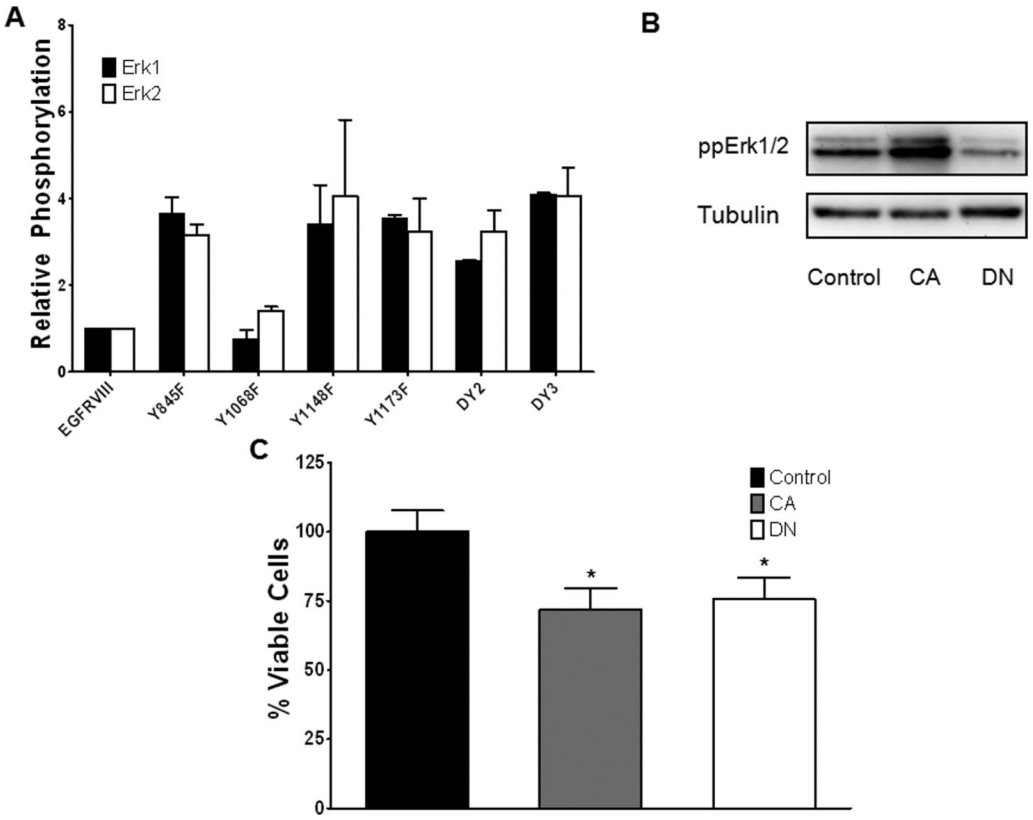

Figure 5. Phenotypic responses of U87MG-EGFRvIII cells to Erk modulation

(A) Relative phosphorylation levels of Erk1 (T202/Y204) and Erk2 (T185/Y187) in EGFRvIII mutant cell lines. Phosphorylation levels are normalized to the U87MGEGFRvIII control cell line with error bars representing data from biological replicates. (B) Western blot of double phosphorylated Erk1/2 after transfection of U87MGEGFRvIII cells with either pBabe-puro (Control), constitutively activate MEK (CA) or dominant negative MEK (DN). (C) Viability response of U87MG-EGFRvIII cells upon modulation of the Erk pathway. Transfected cells were subjected to serum deprivation conditions for 72 hours prior to counting viable cells by trypan blue exclusion method. Experiments were performed in 6 replicates normalized to control cells. *$p<0.01$.

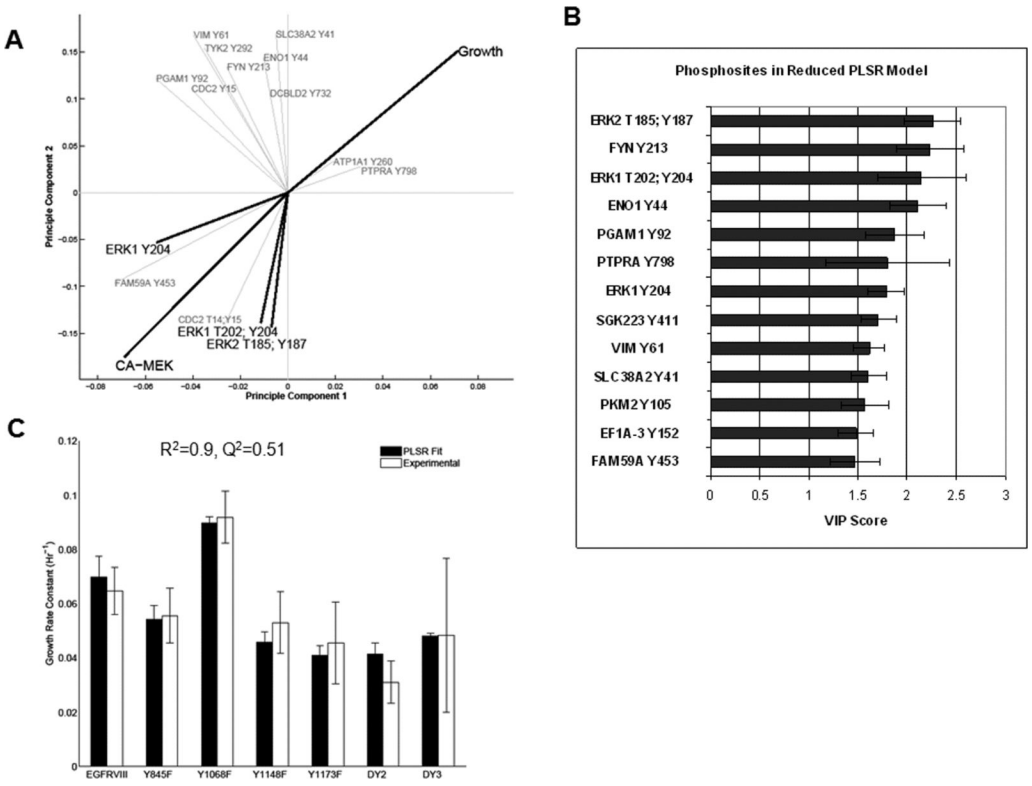

Figure 6. PLSR visualization of Cell Viability, CA-MEK and reduction of PLSR GBM cell growth model

(A) Contributions of cell viability under CA-MEK, growth, and phosphorylation sites are plotted onto their corresponding 2D PLSR principle component axes. The phosphosites with the ten highest variable importance of projection scores are plotted in the figure. CA-MEK viability clusters with Erk1/2 phosphosites and opposite growth. (B) Variable importance for projection (VIP) of the thirteen phosphosites included in the Reduced PLSR U87 Cell Growth Model. Errors bars were estimated using leave-one-out cross validation methods. (C) Fit of the Reduced PLSR U87 Cell Growth Model to the exponential growth rate constants. Error bars for experimental and PLSR fits represent standard deviations as estimated by maximum likelihood or leave-one-out-cross-validation methods, respectively.

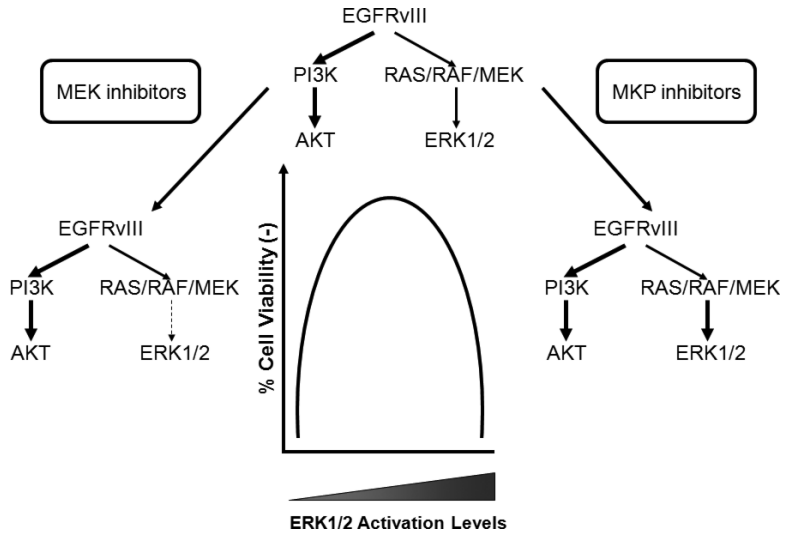

Figure 7. Schematic of dependence of EGFRvIII-expressing cells on Erk 1/2 activation

EGFRvIII represses the Erk pathway and preferentially activates the PI3K/Akt pathway, thereby achieving optimal cell growth. Modulation of the Erk pathway through MEK inhibition (decreasing Erk activation) or MAPK-phosphatase (MKP) inhibition (increasing Erk activation) decreases cell viability, providing two potential methods for decreasing glioblastoma cell growth for those GBMs expressing EGFRvIII.